Optimal Placement of Fiber Optic Sensors for Deposit Growth Monitoring in Process Furnaces

Samir Cerimovic
Dept. for Integrated Sensor Systems
Danube University Krems
Wiener Neustadt, Austria
samir.cerimovic@donau-uni.ac.at

Thilo Sauter
Dept. for Integrated Sensor Systems
Danube University Krems, and
Institute of Computer Technology
Vienna University of Technology
thilo.sauter@donau-uni.ac.at

Albert Treytl
Dept. for Integrated Sensor Systems
Danube University Krems
Wiener Neustadt, Austria
albert.treytl@donau-uni.ac.at

Rudolf Stachl
Fiber Cable Technology
NBG
Gmünd, Austria
r.stachl@nbg.tech

Joachim Binder
Fiber Cable Technology
NBG
Gmünd, Austria
j.binder@nbg.tech

Petar Basic
STE
Split, Croatia
p.basic@ste.hr

Franz Mehofer
OMV
Schwechat, Austria
franz.mehofer@omv.com

Ernst Schober
OMV
Schwechat, Austria
ernst.schober@omv.com

Sherry Rinsche
OMV
Schwechat, Austria
sherry.rinsche@omv.com

2021 IEEE 30th International Symposium on Industrial Electronics (ISIE) | 978-1-7281-9023-5/21/$31.00 ©2021 IEEE | DOI: 10.1109/ISIE45552.2021.9576302

***Abstract*—The growth of deposit layers in process furnaces is an inevitable problem in industrial processes. Monitoring this process in a non-invasive, model-based manner can help to improve process quality and extend runlength between maintenance cycles. A key parameter in this context is the outer pipe wall temperature. Contrary to common spot temperature measurements, we propose fiber optic sensors (so-called Fiber In Metal Tube, FIMT) allowing a high spatial resolution. The exact location of the FIMTs is decisive for the sensitivity of the temperature measurement. Since our test facility is a high-temperature furnace, the optimal FIMT position cannot be evaluated experimentally in the usual manner. Therefore, we present a model-based approach taking into account the thermal characteristics of the deposit layer, the turbulent hot air flow inside the chamber and also imperfections of the FIMT installation such as non-ideal thermal contacts. 2D FEM simulations show the temperature distribution around the pipes and are used to indicate best positions regarding the optimal mounting of the sensors.**

Keywords—deposit detection, distributed fiber-optics, high-temperature measurements, FEM simulations, FIMT

I. Introduction

Gradually growing deposits on the inside of pipe walls can be a major issue in many industrial processes. They reduce the usable pipe diameter, in extreme cases cause pipe blockages, and generally deteriorate process quality and efficiency. Removal of such deposits is complicated and costly [1]. Even though deposit growth is unavoidable in many cases due to the nature of the process, understanding and controlling it is beneficial to extend unit runlengths and maintain or improve process quality. The fundamental problem is that the thickness of the deposit layer is typically not directly measurable, so model-based estimation approaches that use process variables and parameters that are accessible from the outside of the pipe must be employed.

In the case of process furnaces in petrochemical industry investigated in this paper, the hypothesis is that the deposit layer influences the thermal properties of the pipe and therefore the heat transfer process. This should be visible in the surface temperature of the pipe wall, in the sense that a thicker deposit layer impedes the heat transfer into the pipe and therefore leads to higher surface temperatures. To that end the surface temperature must be monitored, which is most easily done with state-of-the-art thermocouples [2, 3] at few selected positions. However, given that the deposit growth cannot be assumed to be homogeneous along the pipes, the value of spot measurements is questionable.

In order to gain deeper insight into the deposit formation, temperature measurements with finer spatial resolution are needed. Glass-fiber-based temperature sensing systems are a logical choice [4]. A single passive, high-temperature glass fiber allows measurements with a spatial resolution in the range of 10 cm and a temperature resolution of up to 0.1°C [5]. However, the highest temperatures that can be measured using conventional optical fiber technology are limited to around 300°C. In many petrochemical facilities the process temperatures can be more than twice as high. Therefore, the fibers must be additionally protected, for instance with metallic coatings like gold or copper. In addition, and also to ease handling, the fiber can be placed in small metal tubes. This technique is called FIMT (Fiber In Metal Tube) and can extend the measurement range to over 700°C, which is sufficient for the most petrochemical processes.

Fig. 1 shows a schematic sketch of the sensing principle. Inside a furnace a hot gas flow heats the outer wall of the vertically arranged pipes. The heat transferred to a fluid

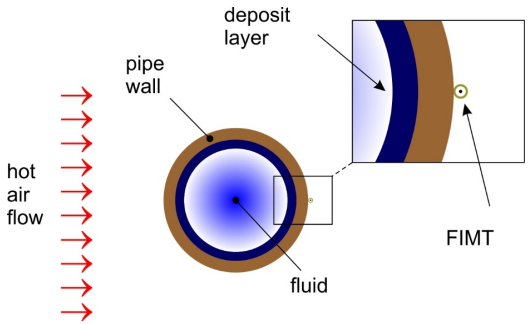

Fig. 1. Schematic cross-section through a pipe inside of a heat exchanger chamber. A "Fiber In Metal Tube" (FIMT) measures the outer wall temperature to detect the thickness of the deposit layer.

The work reported in this paper is partly funded by the state of Lower Austria under the detect.it project.

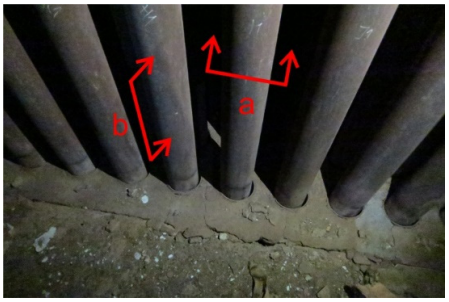

Fig. 2. Pipe elements in the cracking furnace of the test facility. The photo shows only one row of pipes. The red arrows indicate the sections that are taken into account in the 2D modeling.

triggers petrochemical cracking processes inside the pipes. The gradually growing deposit layer on the inner pipe wall acts as an insulation layer between the pipe wall and the fluid. Thus, the thickness of the deposit layer can be detected indirectly by placing the FIMT in an appropriate position and measuring the outer wall temperature [6].

Extending preliminary work reported in [6], this paper primarily addresses the question where to position the fiber optical sensors in order to achieve robust measurements, also taking into account limitations of practical installation. This is done by investigating simplified finite element models for the essential heat transfer mechanisms.

II. FEM Modeling

The use case serving as a model is a petrochemical cracking furnace in a refinery. In this furnace, a hot air flow of up to 600 °C heats the fluid (essentially relatively viscous residues from crude oil distillation) flowing through a bundle of parallel pipes as depicted in Fig. 2.

The FIMTs should be mounted along the pipes using suitable mounting brackets. The exact location of the FIMTs is decisive for the sensitivity of the temperature measurement. Since the test facility is a high-temperature production plant that can only be switched off and entered for maintenance purposes at planned unit shut downs, the optimal location of the FIMTs cannot be determined experimentally. Instead, numerical simulations based on the finite element method (FEM) must be used.

The crucial aspect for the modeling is that in the chamber, two orthogonal fluid flows interact: the hot air flow outside and the fluid flow inside the pipes (cf. also Fig. 1). Such configurations can be comprehensively modeled only by implementing a three-dimensional (3D) approach. However, 3D simulations are very memory- and time-consuming. Fortunately, some very important questions, such as optimal position of the FIMTs, can also be answered by applying two-dimensional (2D) models. For that purpose, the complex 3D model must be split in two simple 2D models.

The geometry of the first 2D model stems from the horizontal cross-section in the middle of the chamber as indicated in Fig. 2 by letter “a”. The same geometry is also schematically depicted in Fig. 1. This 2D model can be used to predict the velocity field of the hot air flow, the pipe wall temperature, and the temperature distribution around the pipes. A prerequisite is, however, the knowledge about how the fluid flow inside the pipe influences the wall temperature.

The hot air in the furnace heats up the outer surface of the pipes, whereas the inner surface is cooled by the fluid flowing inside. This is similar to a heated surface being convectively cooled by the passing fluid flow. This convective cooling aspect can be modeled by specifying two essential parameters: the heat transfer coefficient h and the fluid temperature in the middle of the pipe as a boundary condition.

The heat transfer coefficient depends on the thickness of the deposit layer d – the thicker this layer, the smaller the inner diameter of the pipe. This in turn influences the mean flow velocity inside the pipe as well as the Reynolds number, and consequently also the heat transfer coefficient h.

In order to estimate the influence of the fluid flow inside the pipe and its dependence on the deposit layer thickness, another 2D model must be developed. The geometry of this second 2D model is derived from the vertical cross-section through a single pipe as indicated by letter “b” in Fig 2. Due to rotational symmetry, it is sufficient to consider only the space between the pipe axis and the outer pipe wall. This model shown in Fig. 3a will be described in more detail below.

A. 2D model for estimation of the heat transfer coefficient

While in reality the fluid in the pipe is a two-phase mixture of a liquid and a gaseous component, we assume for simplicity reasons a conventional single-phase flow with averaged material parameters (density, viscosity and heat capacity) calculated according to the distribution of the individual phases. The resulting fluid exhibits a turbulent flow profile according to

$$u = u_{max}\left(1-\frac{r}{R}\right)^{\frac{1}{n}}, \text{ with } u_{max} = \overline{u}\cdot\frac{2n^2+3n+1}{2n^2}. \quad (1)$$

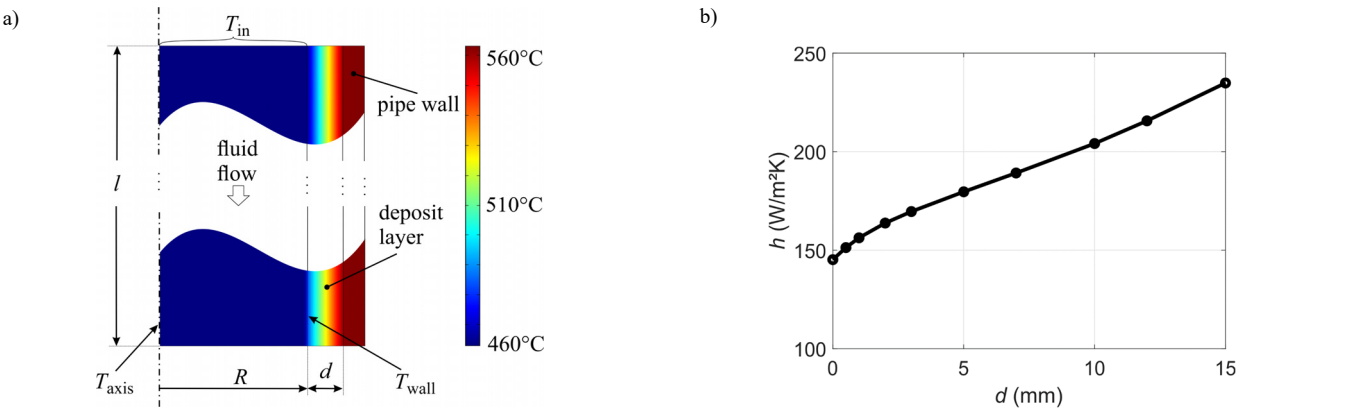

Fig. 3. a) 2D rotationally symmetric model used for the estimation of the heat transfer coefficient h. The thickness of the deposit layer d was varied between 0 mm and 15 mm (here d = 10 mm). b) Dependence of the heat transfer coefficient h on the thickness of the deposit layer d.

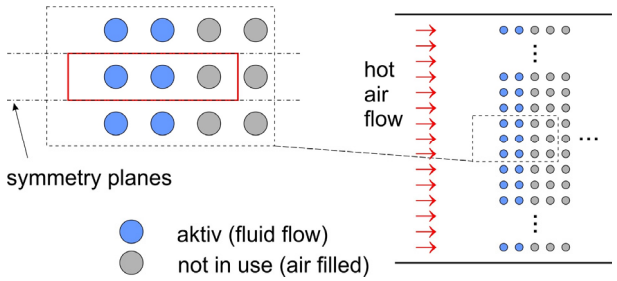

Fig. 4. Schematic sketch of the cracking furnace serving as a test facility. The red frame in the inset indicates the geometry used for 2D modeling.

Here, $n = 10$ for highly turbulent flow, and $\overline{u}$ represents the average flow velocity that can be calculated from the volume flow $\dot{V} = R^2 \cdot \pi \cdot \overline{u}$. The latter is assumed to be constant in the order of 0.1 m³/s. Depending on the deposit layer thickness d and hence on the inner pipe radius R, we calculate the average flow velocity $\overline{u}$ and the maximum velocity $u_{\max}$ in the middle of the tube.

Fig. 3a shows the rotationally symmetric 2D model. We assume that the pipe is heated uniformly from all sides by the hot air flow, i.e., the temperature on the outer pipe wall is specified as a boundary condition $T_{\text{air}} \approx 560°\text{C}$. In order to calculate the heat transfer coefficient, we first simulate the total heat transfer rate

$$\dot{Q} = \iint q \mathrm{d}A\,, \tag{2}$$

where q is the heat flux perpendicular to the pipe surface. The heat transfer coefficient h results then from

$$h = \frac{q}{\Delta T} = \frac{\dot{Q}}{A_{\text{wall}} \cdot (T_{\text{wall}} - T_{\text{axis}})}\,, \tag{3}$$

with $A_{\text{wall}} = 2R\pi l$ as the inner surface of the pipe and $l = 10$ m as the length of a single pipe element (see. Fig. 2). The fluid temperature at the pipe inlet is assumed to be a hundred degrees below the air temperature (i.e., $T_{\text{in}} \approx 460°\text{C}$). $T_{\text{axis}} = \int_0^l T(r=0)\mathrm{d}z$ is the average temperature along the axis of rotational symmetry ($r = 0$). Since only a relatively thin fluid layer near the wall is heated, $T_{\text{axis}} = T_{\text{in}}$ always holds. $T_{\text{wall}} = \int_0^l T(r=R)\mathrm{d}z$ denotes the average temperature along the inner wall ($r = R$).

Fig. 3b shows the simulated dependence of the heat transfer coefficient h on the thickness of the deposit layer d. These values were used for the subsequent simulations.

B. 2D model for simulation of the temperature distribution

After the effect of the flowing fluid on the wall temperature has been quantified, the actual 2D model for simulation of the temperature distribution around the pipes can be developed. As mentioned above, it is modeled from the horizontal cross-section in the middle of the furnace. The first step is to determine the necessary model geometry.

Fig. 4 depicts a schematic sketch of the furnace. In the test facility, not all pipes are actually "active", i.e., filled with the flowing fluid. For technical reasons, some pipe rows are not in use. They are disconnected from the rest of the pipes using a bypass system and contain just resting air (neglecting natural convection).

In order to confine the model geometry, the planes of symmetry must be identified. As the fluid flows through the pipes, it absorbs the heat and its temperature gradually rises towards the outlet. So each pipe features a different temperature. Nonetheless, we can assume that at least the neighboring pipes are approximately at the same temperature. Thus, the temperature distribution between the pipes is approximately symmetrical, with planes of symmetry running exactly in the middle between the respective pipes. The distance between two adjacent planes of symmetry determines the width of our 2D model (see the inset of Fig. 4).

In preliminary simulations, the necessary length of the 2D cross-section was investigated in order to simplify the model geometry as much as possible. It was found that an inlet distance of about 30 cm is sufficient. The preliminary results also show that only the first row of "inactive" pipes has to be considered. Taking into account subsequent pipe rows would not influence the temperature distribution around the first two "active" rows of pipes. Finally, an outlet section of about 30 cm after the third pipe row turned out to be fully adequate.

Fig. 5 shows the actual 2D model that is used for the temperature distribution around the pipes. The limitation to 2D modeling is justified, as the pipes are 10 m long, while the outer diameter amounts to slightly more than 11 cm, i.e., the aspect ratio is very large. In addition, the air flow is turbulent, i.e., the mean flow velocity in the middle of the furnace (simulation level) does not deviate much from the value at the edges (as it would be the case with a laminar flow). Therefore, the restriction to 2D is a good approximation that enormously reduces the complexity or computing effort compared to 3D simulations.

The 2D geometry results from a cross-section in the middle of the furnace (this area is indicated with a red frame in the inset of Fig. 4), and it is assumed that the temperature and flow velocity field do not change in z-direction (perpendicular to the simulation plane), i.e., as if the pipes were extended indefinitely. Due to reasons mentioned above, this is a reasonable approximation, apart from the areas in the immediate vicinity of the top and bottom wall of the furnace.

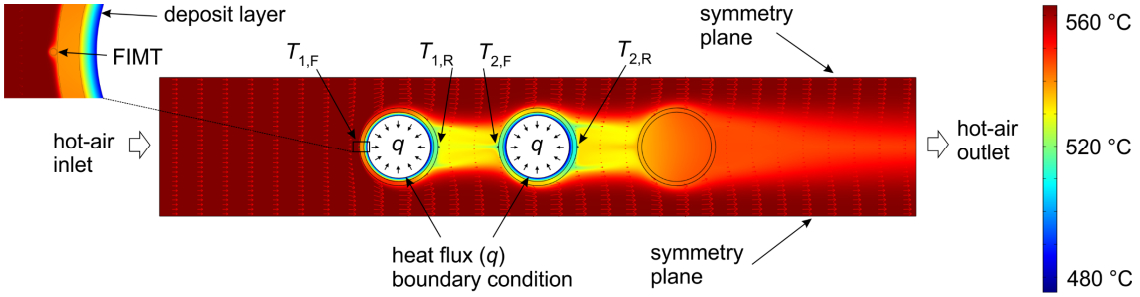

Fig. 5. 2D model for simulation of the temperature distribution with FIMTs (inset left). The FIMTs are placed on the front and the rear of the pipes. For the simulation, a 5 mm thick deposit layer was chosen. Red arrows indicate the flow velocity field.

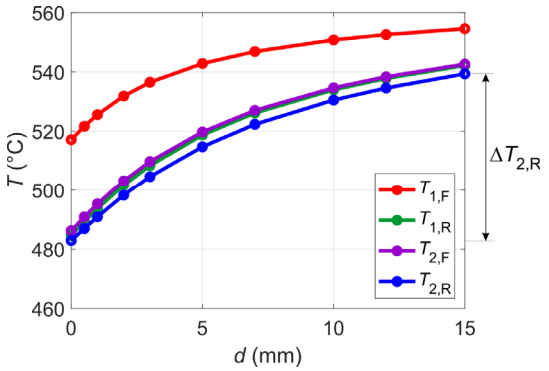

Fig. 6. Fiber temperature as a function of the deposit layer thickness d for different positions of the FIMTs.

Commercial multiphysics FEM simulation tools enable modeling of arbitrary coupled physical processes. In our case, the heat transfer is coupled with the fluid flow. The extremely turbulent hot air flow around the pipes was modeled applying k-ω module of the simulation tool. Here, the very thin viscous sublayer next to the wall and the adjacent buffer layer are neglected, and a special wall function is used to analytically compute a nonzero fluid velocity directly at the wall. The flow field in the adjacent log-law and free-stream flow regions is then computed with the help of the Reynolds-averaged Navier-Stokes (RANS) model [7]. An average hot air velocity of $\bar{u}_{\text{in}} = 5$ m/s was specified as the inlet boundary condition, while the outlet was set to zero pressure. The red arrows in Fig. 5 denote the resulting flow velocity around the pipes.

The convective cooling of the pipes by the viscous fluid mixture flowing inside is modeled as a boundary condition with heat flux q, where the fluid temperature in the center of the pipe T_{axis} and the heat transfer coefficient h (taken from Fig 3b) must be entered as parameters. The inlet was set to the constant temperature condition of $T_{\text{air}} \approx 560\,°\text{C}$, while the outlet is modeled as a boundary condition with convective heat flux.

III. Simulation of FIMT Temperature

For simplicity reasons, the FIMTs are modeled as small metallic tubes filled with resting air (see inset on the left side of Fig. 5). Based on initial considerations about the practical installation of the FIMTs, four positions are investigated at the front (index F) and rear (index R) of the pipes. The temperature of the respective FIMT is then determined by the integration over the inner surface of the tube $T_i = \iint T \mathrm{d}A$, where index i indicates the position.

Fig. 6 shows the dependence of the FIMT temperature on the deposit layer thickness d for different positions of the FIMTs. Supporting the initial hypothesis, a thicker deposit layer leads to a higher thermal insulation of the pipe and consequently shields the pipe wall from the convective cooling by the fluid in the pipe. This increases the temperature on the outer wall of the pipe. This effect obviously depends on the position of the FIMTs. The absolute temperature is highest at the front of the first pipe because this position is most exposed to the hot air flow. On the other hand, the goal of the temperature monitoring is to observe the deposit growth. Therefore, we are interested in the sensitivity, which is related to the difference $\Delta T = T_{15\text{mm}} - T_{0\text{mm}}$ between the temperature at maximum ($d = 15$ mm) and minimum ($d = 0$ mm) layer thickness. Fig 6 shows this difference at the rear of the second pipe ($\Delta T_{2,\text{R}}$). Similar values appear in between the pipes, i.e., on the front of the second ($\Delta T_{2,\text{F}}$) and the rear of the first pipe ($\Delta T_{1,\text{R}}$). The front position of the first pipe apparently is the least sensitive one.

IV. Investigation of the Optimal FIMT Position

With a view to the installation of the monitoring system, it is important to know which positions are best suited for FIMT installation and how sensitive these locations are with respect to inevitable deviations from the ideal position. To that end, we simulated the temperature along the outer wall of the pipes with and without deposit layer ($d = 15$ mm and $d = 0$ mm, respectively). Due to the symmetry of the model, only the upper half of the model depicted in Fig. 5 needs to be considered (see inset in the upper part of Fig. 7). Simulations were performed without FIMTs because their influence on the temperature field can be neglected.

Fig. 7 illustrates the results, showing the dependence of the surface temperature on the polar angle. As expected, temperatures without deposition ($d = 0$ mm, blue curve), are significantly lower than with maximum deposition ($d = 15$ mm, red curve). In the latter case, the isolation effect is more pronounced, and the actual position of the FIMTs is less critical (the red curves become flatter). What counts for the selection of the best position, however, is the difference

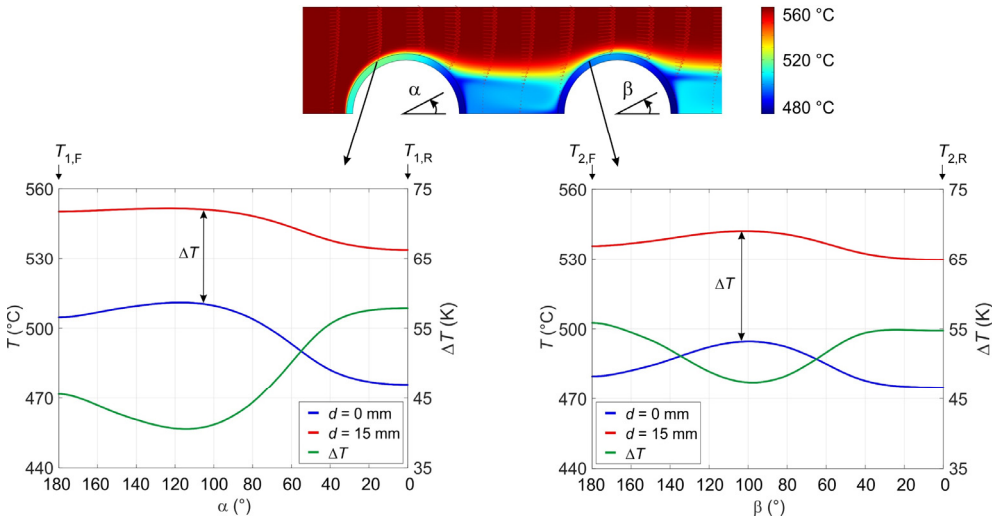

Fig. 7. Surface temperature as a function of the polar angle for the cases without deposition ($d = 0$ mm) and with the maximum deposit layer thickness ($d = 15$ mm). The inset above shows simulation result for the pipes without deposit layer (corresponds to the blue curve in the diagrams).

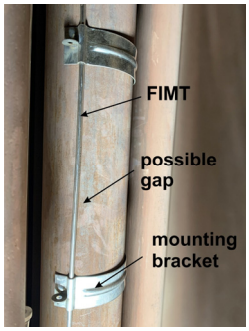

Fig. 8. FIMT mounted on the pipe surface using metal brackets. Due to mechanical reasons a small gap between the two can occur.

between the two curves ΔT (green curve in Fig. 7), indicating the sensitivity of the monitoring system to deposit growth.

In accordance with the results from Fig. 6, the highest sensitivity is achieved at the rear side of each pipe, which is a "flow shadow" area not directly exposed to the hot air flow. About $\pm 30°$ away from these points, the temperature difference becomes increasingly lower, reaching a minimum at around 100°. At this point, the average velocity of the air flow is highest, and the outside heating effect from the hot air becomes dominant over the cooling inside. Another advantageous position would be the front of the second pipe, which is still within the "flow shadow" of the first pipe. Conversely, the front side of the first pipe is, as seen before, a very insensitive position and only marginally better than the worst case around the polar angle of 100°.

A closer inspection of Fig. 6 at $d = 0$ and Fig. 7 for the case without deposits (also $d = 0$) reveals that the temperatures in Fig. 6 are somewhat higher. This difference stems from different simulation setups: For Fig. 7, we evaluated the surface temperature of the pipes, whereas Fig. 6 shows the mean temperature of the FIMTs. As the inner area of the FIMTs is slightly off the outer pipe wall (see inset of Fig. 5), the FIMT temperature is also slightly higher. However, the two figures are qualitatively equivalent in that $T_{2,R}$ exhibits the lowest value, followed by $T_{1,R}$ and $T_{2,F}$, and finally $T_{1,F}$ showing the largest temperature.

V. Simulation of the Thermal Coupling Effects

An important practical aspect for the functioning of the fiber optic sensing system is the thermal coupling between a FIMT and the pipe. The simulations so far assumed a good contact between the two objects. In practice, however, this cannot be guaranteed. Fig. 8 shows the mounting of a FIMT using metal brackets. Only around the mounting brackets an ideal thermal coupling can be guaranteed. Elsewhere we may expect a small gap between the pipe surface and the FIMT, which will have an impact on sensitivity.

FEM simulations can help to quantify this effect. We estimated that the maximum gap could amount to about 5 mm. Therefore, we first simulated the temperature along semicircles 5 mm away from the outer surface of the pipes. The simulation results are illustrated in Fig. 9. Similar to previous simulations without the gap (see Fig. 7), we considered the cases without deposition ($d = 0$ mm, blue curves) and with the maximum deposit layer thickness ($d = 15$ mm, red curves). The difference between these characteristics ΔT is again a measure for the sensitivity of the fiber optic sensing system (brown curves in Fig. 9).

Simulation results for the first pipe reveal the lowest sensitivity in the area where $\alpha > 90°$. Here, the FIMT is hit frontally by the hot air flow and its temperature lies around the ambient temperature ($T_{air} \approx 560$ °C), independent of the deposit layer thickness. Thus, the FIMT temperature without deposition ($d = 0$ mm) and with the maximum deposit layer thickness ($d = 15$ mm) are almost the same in this area and ΔT tends to zero. A similar effect, however not so pronounced, can be observed for the second pipe in the range of $80° < \beta < 120°$, i.e., on the side facing the unobstructed air flow. In the "flow shadow" areas (rear side of the pipes and front side of the second pipe), however, there are noticeable temperature differences induced by the deposit layer even 5 mm away from the pipe surface.

In order to determine the FIMT mounting areas on the pipe surface that are less sensitive to possible gaps, the comparison between simulation results for cases with and without the gap can be useful. This is depicted in Fig. 10. It should be pointed out again that we considered only the worst-case scenario with the maximum gap of 5 mm. In the reality, smaller distances, in the range of 1 mm or even less, can be expected. Thus, the gap impact should be less dramatic, as predicted by the FEM simulation results. According to Fig. 10, there are three possible mounting positions where the sensor sensitivity with the gap is almost the same as without it, i.e., the impact of the

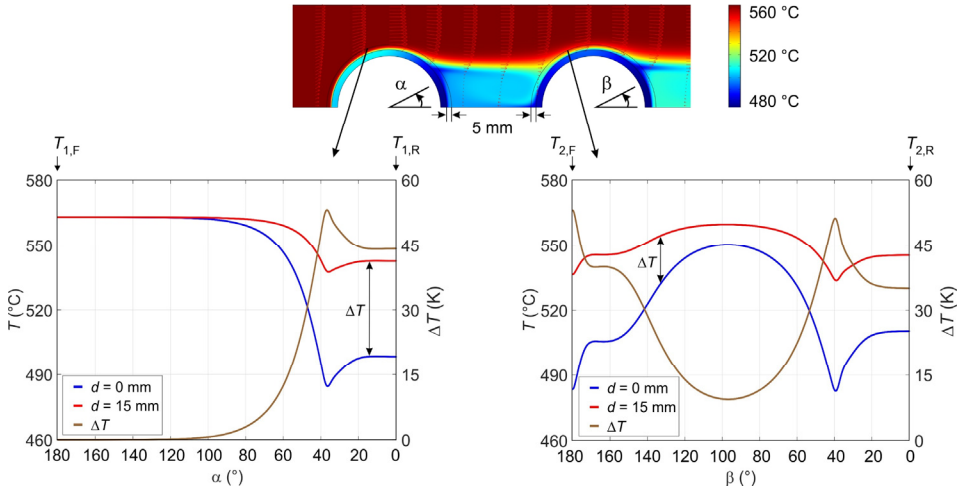

Fig. 9. Temperature along semicircles 5 mm away from the pipe surface as a function of the polar angle for the cases without deposition ($d = 0$ mm) and with maximum deposit layer thickness ($d = 15$ mm). The inset above shows simulation result for the pipes without deposit layer (corresponds to the blue curve in the diagrams).

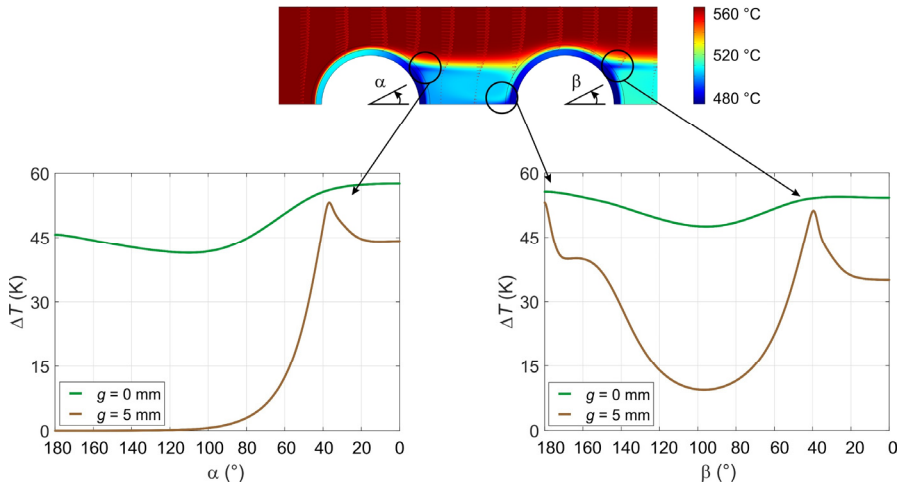

Fig. 10. Comparison of the temperature difference ΔT for the cases without the gap (g = 0 mm) and the maximum gap width of g = 5 mm as a function of the polar angle.

gap can be neglected. For both pipes, these locations can be found at a polar angle of about 40°. Additionally, for the second pipe, a good position to place a FIMT would be at the front of the pipe at β = 180°.

The optimal mounting locations are marked with a circle in the inset of Fig. 10. Due to eddy formation, these areas are cooler than the rest of air flow near the pipe surface (dark blue color in the inset of Fig. 10). Here, the main effect determining the FIMT temperature is the convective cooling by the flow inside the pipe, rather than the hot air flow around the pipe.

The precise position of the sharp peaks of the ΔT characteristics for g = 5 mm (around 40° in Fig. 10) depends on the velocity of the hot air flow and on the grade of turbulences. If the flow regime changes, the peaks could be shifted. Therefore, it would be wrong to speak about strict optimal positions for the mounting of the FIMTs at the rear of the pipes. Instead, we can conclude, that areas with a polar angle below 40° feature good sensitivity and low dependence on the width of the possible gaps. Moreover, another advantageous location, as mentioned above, can be found at the front of the second pipe, around β = 180°. All other areas at the pipe circumference should be avoided when mounting the FIMTs.

VI. Conclusion and Outlook

The preliminary results and considerations presented in this paper are naturally based on data from a specific petrochemical plant, but the general approach is applicable to other industrial processes as well. Deposition layers in process furnaces are a common problem, and a model-based concept to monitor and possibly predict their growth can help to improve plant operation and process quality. The distributed temperature measurement based on fiber optical sensors proposed here is probably too complex as a standard process monitoring solution, but is expected to give insight into the question whether or not the deposit layer thickness is homogeneous or at least monotonic along the pipes.

The second aspect in this paper concerned the optimal placement of the fiber optical sensors. Since a full 3D modeling is too resource consuming, the models had to be simplified. This and the fact that turbulent flows are generally difficult to simulate mean that the absolute temperature values obtained from the simulations should be treated with caution. Nevertheless, what is relevant for answering the question where the sensors should be mounted is not so much the absolute values but the sensitivity, i.e., the range of the measured temperature depending on the thickness of the deposit layer. These qualitative results can be considered reliable for the further course of the research. In particular, we could also answer a serious practical question that arose in first test installations: For simple mechanical reasons, it cannot be guaranteed that the sensor tubes have perfect thermal contact with the pipes they are mounted on. A small gap will be almost inevitable, at least along parts of the installation. Interestingly, the simulation results indicated that there are locations where the sensitivity of the sensor with and without air gap is comparable.

Future work will consider a more complex 3D model as well as detailed investigations of the two-phase flow. Moreover, a model describing the correlation between the pipe surface temperature and the thickness of the deposit layer must be developed. Finally, the results of this comprehensive modeling will be compared with data gained by the in-situ measurements in the test facility.

References

[1] A.F. Stam, W.R. Livingston, M.F.G. Cremers, and G. Brem, “Review of models and tools for slagging and fouling prediction for biomass co-combustion,” Review article for IEA 2010; Task 32; 2010. pp. 1–18.

[2] A.B. Hopwood, S. Chynoweth, and G.T. Kalghatgi. “A Technique to Measure Thermal Diffusivity and Thickness of Combustion Chamber Deposits In-Situ,” *SAE Transactions* 107, 1998, pp. 596-605.

[3] Q. Xiaobin, S. Guoliang, S. Weijian, Y. Shaobo, and L. Qinggang, “Effects of wall temperature on slagging and ash deposition of Zhundong coal during circulating fluidized bed gasification,” Applied Thermal Engineering, Vol. 106, 2016, pp. 1127-1135.

[4] J. W. Berthold, L. A. Jeffers and R. L. Lopushansky, “Fiber optic sensors for the refinery of the future,” 2nd ISA/IEEE Sensors for Industry Conference, Houston, TX, USA, 2002, pp. 40-43.

[5] T. Landolsi and A. Kaye, “Oil Refinery Monitoring Using Fiber-Optic Distributed Strain And Temperature Sensors”, White Paper, OZ Optics, www.ozoptics.com/ALLNEW_PDF/APN0016.pdf, Juni 2020.

[6] S. Cerimovic et al., “Measuring Temperature Distributions along Heat Exchanger Pipes in Petrochemical Processes,” 25th IEEE International Conference on Emerging Technologies and Factory Automation (ETFA), Vienna, Austria, 2020, pp. 1347-1350.

[7] W. Frei, “Which Turbulence Model Should I Choose for My CFD Application?”, COMSOL (2017), www.comsol.com/blogs/which-turbulence-model-should-choose-cfd-application, Juni 2020.